

Liquid Crystal Director Dynamics Imaged Using Two-Photon Fluorescence Microscopy with Remote Focusing

P. S. Salter,* G. Carbone, E. J. Botcherby, T. Wilson, S. J. Elston, and E. P. Raynes

Department of Engineering Science, University of Oxford, Parks Road, Oxford, OX1 3PJ, United Kingdom

(Received 17 July 2009; published 18 December 2009)

We introduce a novel imaging technique adopting remote focusing for resolving the axial dynamics in the director field for liquid crystals. The high axial time resolution of our approach is demonstrated by imaging directly the evolution of the director field for an initially splayed nematic layer subject to a sudden voltage pulse. Images of the switching dynamics are presented, revealing transient state director configurations and changes in topology of the liquid crystal layer.

DOI: 10.1103/PhysRevLett.103.257803

PACS numbers: 61.30.Eb, 42.70.Df, 42.79.Kr

A nematic liquid crystal (LC) is a complex fluid that lacks long range translational ordering, but does possess a degree of orientational order. The nematic alignment is characterized by the director field $\hat{\mathbf{n}}(\mathbf{r})$, which, for common calamitic (“rod-shaped”) materials, describes the local thermodynamic average orientation of the long molecular axis. Knowledge of the director field is an important step in understanding the behavior of a particular system. However, due to the fluid nature of the phase, the director field is free to vary with time, in response to applied external fields or induced flow. The study of director dynamics has developed into a field of wide scientific interest, in part due to the significant technological consequence. The capabilities of director simulations are continually evolving, and can easily predict the dynamic configurations adopted by various LC devices. However, there is as yet no convenient mechanism for direct experimental observation of the axial director dynamics.

Historically, polarizing optical microscopy (POM) has been widely employed in the study of LC dynamics, benefiting from a high temporal resolution. However, the technique provides only an integrated two-dimensional image of the LC layer and yields no explicit information on the director orientation at a particular depth. In recent years fluorescence confocal polarizing microscopy (FCPM) [1] has developed into a useful tool for three-dimensional imaging of the LC director configuration [2]. A Nipkow-disk scanning confocal microscope can be used to image dynamics in the plane of a device [3], but axial scanning is more complicated since the motion of the sample in refocusing is intrinsically slow and additionally would produce flow that might affect the director distribution. Here we employ two-photon fluorescence microscopy (TPFM) [4] with remote focusing [5] to determine the director structure of a nematic layer. The remote focusing of the system avoids any mechanical agitation of the sample and enables high axial scan speeds throughout the depth of the layer, allowing imaging of dynamic variation in the director.

As an example, we consider the axial dynamics of a nematic layer subject to the sudden application of a trans-

verse electric field. In the zero-field H state a uniform splay distortion of the director is imposed on the layer by a small pretilt at each surface (a π cell [6]). Applying an electric field perpendicular to the substrates a series of transitions through different states are observed as outlined in Fig. 1. The dynamics of this system present an interesting study, due to the variety of its transient, stable and metastable states prompting significant prior attention [7–13].

The director for materials with a positive dielectric anisotropy tends to align parallel to an applied field, subject to the constraints imposed by the surfaces. At the midpoint of a π cell, the director is initially parallel to the substrate and, hence, degenerate with respect to tilt direction when reorienting with the field. Thus, the H_s state is formed on field application, characterized by a thin H_s wall of high distortion in the middle of the layer where the director is perpendicular to the field. The H_s state only forms transiently, and with time collapses to either the asymmetric H_a state, or at higher voltages the topologically dissimilar V state, both of which exhibit a lesser degree of elastic distortion. There has been recent interest in the H_s state as both a potential fast-switching display mode [7,11] and as a precursor to the reported bulk order reconstruction across a two-dimensional sheet in the mid-

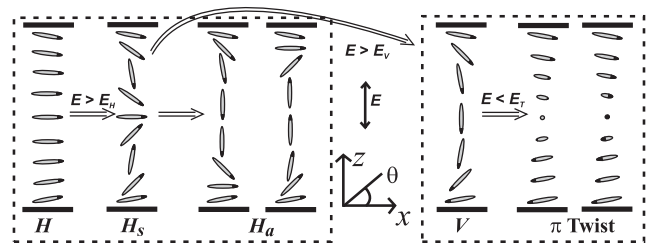


FIG. 1. At zero applied voltage the splayed H state is the ground state in a nematic π cell. Applying an electric field above a certain threshold, the transient H_s state forms prior to relaxation into either of the two possible H_a states, or, at higher voltage, the topologically distinct V state. For a sufficiently low voltage, the H_s and H_a states return to the initial H state while the V state relaxes to a $\pm\pi$ twist.

plane of the LC layer during the transition to the V state [8,9]. Previous studies have indirectly inferred the H_s director profile [10,12], but direct observation of the H_s structure and its evolution has not been possible since any imaging is required to be dynamic; in this letter we apply TPFM with remote focusing to achieve this.

Experimental devices were fabricated with two parallel glass substrates separated by Mylar strips of thickness $30\ \mu\text{m}$. The substrates were spin-coated with polyimide (PI2555-Dupont) alignment layers that were parallel rubbed to provide strong planar anchoring with a pretilt of $\sim 2^\circ$. The upper substrate was $170\ \mu\text{m}$ thick to allow the use of a high-numerical-aperture (NA) oil-immersion objective, while the lower substrate had a thickness of $1.1\ \text{mm}$ to add rigidity to the device. The electrodes on each substrate were $1.2\ \text{mm}$ wide strips of transparent indium tin oxide that overlapped to provide a pixel area of $\sim 1.4\ \text{mm}^2$. The device was filled with the nematic liquid crystal MLC-15900-100 (Merck, $\Delta\epsilon = 10.1$, $\Delta n = 0.091$) doped with a small amount 0.1% w/w of the anisotropic fluorescent dye N,N' -8-bis(2,5-di-*tert*-butylphenyl)-3,4,9,10-perylene dicarboximide (BTBP) from Sigma-Aldrich.

A schematic of the experimental setup is shown in Fig. 2. A Ti:sapphire laser (Tsunami, Spectra Physics) with a wavelength of $850\ \text{nm}$ is operated in a mode-locked regime, which produces pulses of length $100\ \text{fs}$ at a repetition rate of $80\ \text{MHz}$. Although the individual pulses were of high intensity, the average laser power is only $5\ \text{mW}$, which is too low for any optical reorientation effects or melting of the nematic order. The quarterwave plate (QWP) and polarizing beam splitter (PBS) ensure that all light from the laser travels through the system to the sample. The focal

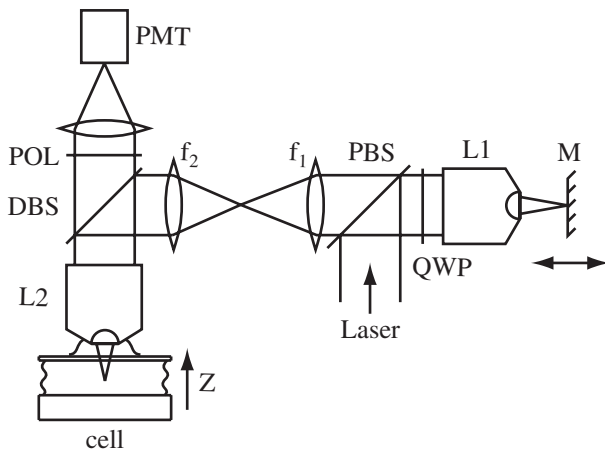


FIG. 2. Setup of the two-photon fluorescence microscope used in scanning the LC layer. An Olympus $0.95\ \text{NA}\ 50\times$ dry objective and an Olympus $1.4\ \text{NA}\ 60\times$ oil-immersion objective were used for L1 and L2, respectively, and their pupil planes were mapped together by a $4f$ imaging system, which is composed of two achromatic doublet lenses with focal lengths $f_1 = 160\ \text{mm}$ and $f_2 = 200\ \text{mm}$.

spot produced by the objective lens L2 can be remotely scanned along the z direction in the sample by moving mirror M , which is mounted on a piezotranslation stage in the focal region of L1. The high-NA objective lens L1 is a key feature of the setup as the refocusing does not introduce any systematic aberration and, hence, diffraction limited resolution is maintained at all points along the axial scan [5].

Dye molecules in the sample are excited by simultaneous absorption of two photons from the laser and subsequently deexcite by emitting a single photon of approximately half the wavelength of the excitation light. The excitation is highest when the polarization of the incident light is parallel to the long axis of the dye molecules. However, if there is an angle θ between the two, the absorption of a single photon is expected to display a $\cos^2\theta$ dependence [1], such that two-photon absorption, and any observed fluorescence, exhibits a $\cos^4\theta$ dependence. Furthermore, two-photon absorption is a weak nonlinear process and the laser intensity is only sufficient for appreciable excitation at the focal spot in the specimen. Therefore any collected fluorescence must originate from the immediate vicinity of the focal point, characterizing the director orientation in just that small volume. The dichroic beam splitter DBS, with cut-off wavelength $750\ \text{nm}$, allowed the fluorescence collected by L2 to be focused onto the photomultiplier tube (PMT) (Sens-Tech Ltd., U.K.). The temporal evolution of the fluorescence was imaged by continuously scanning the focal spot along the z axis and recording the number of photons measured by the PMT at different depths in the sample.

Figure 3 shows images representing the evolution of the LC layer subjected to a burst of oscillating electric field. The polarization of the incident laser is parallel to the surface alignment direction. Therefore, since the dye molecules tend to align parallel to the surrounding LC director [1], regions which are high in fluorescence intensity correspond to the director being largely parallel to the substrate alignment. In Fig. 3, the fluorescence was measured at 100 intervals along the z direction and the integration time, the measurement period for each interval, was set to be $100\ \mu\text{s}$, such that an image of the LC layer was recorded every $10\ \text{ms}$.

Following voltage application in Fig. 3(a), the switched state fluorescence intensity is high near each substrate and also peaks in the middle of the LC layer. This provides the first explicit visualization of the director structure for the transient H_s state, confirming that there is indeed a narrow wall in the LC layer across which the director rotates by $\sim 180^\circ$. The dimension δ of the H_s wall is measured to be $\sim 3.0\ \mu\text{m}$ from the image in Fig. 3(a), while the dielectric coherence length ξ_E , which provides a characteristic length scale for an electric field induced distortion [14], is calculated to be $\sim 1.4\ \mu\text{m}$ for such a voltage. Therefore $\delta \sim 2\xi_E$ as might be expected.

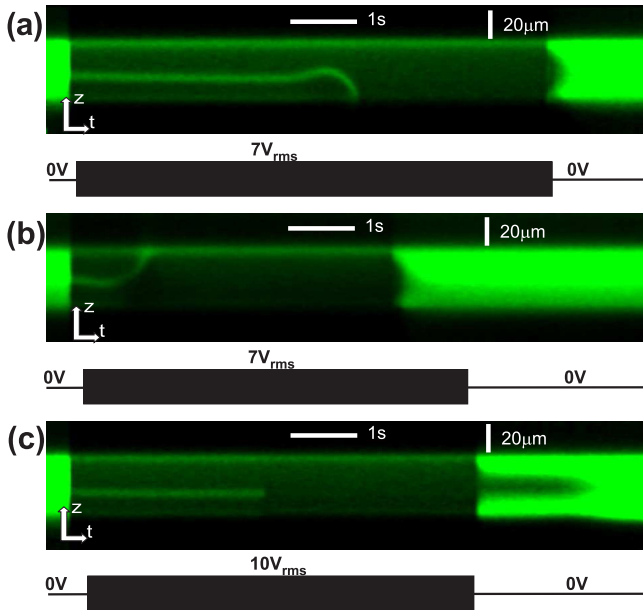


FIG. 3 (color online). Fluorescence images showing the evolution of the LC director field with time, bright regions corresponding to depths in the device where the director is parallel to the substrates.

The H_s wall does not form exactly in the center of the LC layer but is biased toward one substrate, in general at a depth of $0.4d$ from the lower surface, where d is the substrate separation. The position of the H_s wall is dictated by the depth in the device where the director is parallel to the substrate in the field-off H state, and hence degenerate with respect to tilt direction after field application. The observed asymmetry in the formation of the H_s state suggests an inequality in the pretilt of the director at each boundary, with the H_s wall located nearer to the surface with the lower value. Such an effect has been the subject of a recent computational study [13], but never confirmed experimentally. For a net pretilt of 2° , a difference of 0.8° between each substrate, due to the influence of the substrate thickness on the rubbing conditions, would explain the position of the H_s wall. Such asymmetry in the surface conditions breaks the degeneracy between the two possible H_a states and favors the collapse of the H_s state into a particular H_a state over the majority of the pixel, with the H_s wall migrating toward the nearer substrate, as shown in Fig. 3(a). For a purely one-dimensional system, decay to the opposite H_a state would be highly improbable. However, at the electrode edge, the inhomogeneous two-dimensional fringing electric field drives the H_s state into the alternate H_a state as shown in Fig. 3(b), where the central wall is observed to move toward the upper substrate.

In Fig. 3(a), the H_s wall does not collapse directly to the relevant H_a state, but appears to move initially toward the opposite substrate before changing direction. This behav-

ior was observed across a wide range of voltages and at different regions within the pixel area. Such an effect has hitherto never been observed experimentally due to the limits on axial dynamic imaging of the director field nor featured in any prior theoretical modeling of the device switching characteristics. The initial reverse motion in the H_s wall is believed to be a consequence of a complex anisotropic flow field generated by the propagating boundary between the H_s and H_a states.

If a burst of $10 V_{\text{rms}}$ at 1 kHz is applied across the LC layer, as in Fig. 3(c), the formation of the H_s state is seen clearly as before. However, the H_s wall no longer migrates to the substrate and instead decays in the middle of the layer. Such behavior is characteristic of a direct transition from the H_s to V state, facilitated by an order reconstruction of the nematic in the H_s wall. The relatively low electric fields involved here preclude a homogeneous bulk order reconstruction of the form observed elsewhere [8,9], and rather it is confirmed by POM that the transition is mediated by a propagating π disclination line. On removal of the voltage, a two stage relaxation process is evident. Initially a fast transition is observed to the zero-field V state, corresponding to a switch from the dark to bright states in the optically compensated bend mode of a π cell [6]. Subsequently, the nematic layer gradually relaxes into a π twist state. The large value of the Mauguin parameter ($\Delta nd/\lambda$) for the twisted structure dictates that the incident polarization of the excitation beam is guided such that it is parallel to the director at every point in the layer [15], and, therefore, exhibits a uniform fluorescence with depth. However, the π state introduces a different optical aberration to that of the initial H state, such that the fluorescence profiles of the layer prior to and following the voltage burst are distinct, confirming a change in topology of the structure has taken place.

By decreasing the integration time it is possible to increase the temporal resolution in order to focus on the formation and relaxation of the H_s state. In Fig. 4(a), an image of the LC layer is recorded every 2.5 ms during application of a burst of $4 V_{\text{rms}}$ (1 kHz) across the device. Disparity is observed in the switching dynamics above and below the H_s wall at $z(H_s) = 0.4d$. This is emphasized by plotting the fluorescence intensity with respect to time for $z = 0.2d$ and $z = 0.7d$, as shown in Fig. 4(b), indicating that there is a different time constant τ for director reorientation at the two depths. Such behavior is caused by the asymmetry in surface conditions biasing the formation of the H_s wall toward one substrate, effectively creating a situation similar to two parallel devices in the H_a state [7] of differing thickness and, hence, different τ . The experimental data are compared to a theoretical prediction for the evolution in the fluorescence by considering the one-dimensional dynamic variation in the director field based on the balance of viscous, elastic, and dielectric torques. Ignoring any flow effects, the governing equation is

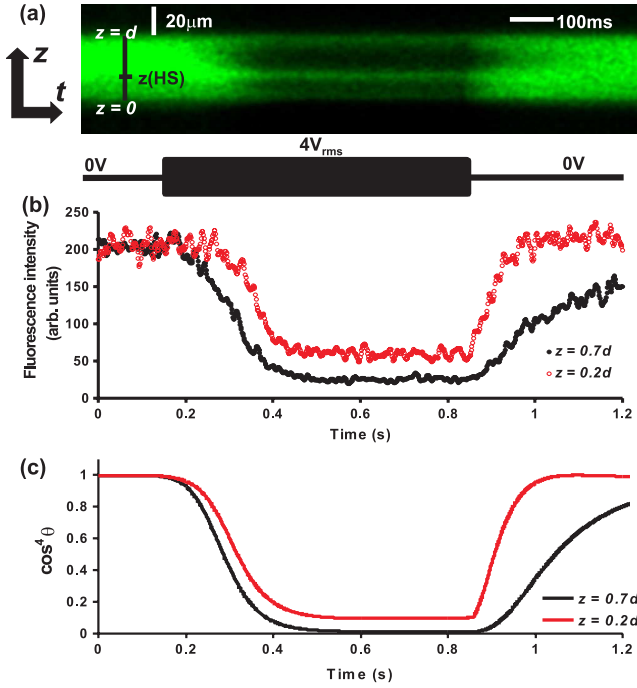


FIG. 4 (color online). (a) Image of the temporal evolution of the fluorescence profile of the LC layer when subjected to a burst of 4 V_{rms} (1 kHz). The fluorescence intensity as a function of time at depths of $z = 0.7d$ and $z = 0.2d$ in the LC layer is plotted from (b) experiment and (c) theory.

$$\gamma_1 \frac{\partial \theta}{\partial t} = (k_{11} \cos^2 \theta + k_{33} \sin^2 \theta) \frac{\partial^2 \theta}{\partial z^2} + \left[(k_{33} - k_{11}) \left(\frac{\partial \theta}{\partial z} \right)^2 + \epsilon_0 \Delta \epsilon E^2 \right] \sin \theta \cos \theta$$

where γ_1 is the rotational viscosity, k_{11} and k_{33} are the elastic constants for splay and bend deformations of the director, $\Delta \epsilon$ is the dielectric anisotropy, and $E(z, t)$ is the local electric field. The surface conditions are set up to provide strong anchoring with a pretilt of $2^\circ \pm 0.4^\circ$ at $z = 0, d$, respectively. Numerical solution to the equation utilizing a relaxation method determines $\theta(z, t)$, and allows us to plot the predicted fluorescence ($\propto \cos^4 \theta$) as a function of time for a particular depth. This is shown in Fig. 4(c), at depths of $0.2d$ and $0.7d$ within the LC layer, where the material parameters $k_{11} = k_{33} = 12$ pN, $\Delta \epsilon = 10$, and $\gamma = 0.1$ Pa s have been employed and a burst of 4 V_{rms} is applied across the device. The theoretical time dependence of the fluorescence during the formation and relaxation of the H_s state displays an excellent correlation with the experimental measurements.

In conclusion, we have presented a novel method to image directly axial dynamics in anisotropic media. The

results presented demonstrate a high degree of temporal and spatial resolution. As an example, the evolution of the transient H_s state in a LC π cell subject to an applied electric field is imaged. The approach gives detailed information on the system dynamics: providing direct verification of theoretical prediction and revealing previously unreported behavior. Aside from TPFM, the method of remote focusing for dynamic imaging is applicable to other techniques used for three-dimensional resolution of a LC director field, such as coherent anti-Stokes Raman scattering [16] and polarized four-wave mixing microscopy [17]. It is hoped that the development of fast axial imaging techniques will provide for a better understanding of dynamic processes in soft matter systems.

The authors gratefully acknowledge the Engineering and Physical Sciences Research Council (U.K.) and Merck for financial support.

*patrick.salter@eng.ox.ac.uk

- [1] I. I. Smalyukh, S. V. Shiyankovskii, and O. D. Lavrentovich, *Chem. Phys. Lett.* **336**, 88 (2001).
- [2] I. I. Smalyukh, *Mol. Cryst. Liq. Cryst.* **477**, 23 (2007).
- [3] I. I. Smalyukh, B. I. Senyuk, M. Gu, and O. D. Lavrentovich, *Proc. SPIE Int. Soc. Opt. Eng.* **5947**, 594707 (2005).
- [4] A. Xie and D. A. Higgins, *Appl. Phys. Lett.* **84**, 4014 (2004).
- [5] E. J. Botcherby, R. Juskaity, M. J. Booth, and T. Wilson, *Opt. Lett.* **32**, 2007 (2007).
- [6] P. J. Bos and K. R. Koehler-Beran, *Mol. Cryst. Liq. Cryst.* **113**, 329 (1984).
- [7] M. J. Towler and E. P. Raynes, in *Proceedings of the 22nd International Display Research Conference (Eurodisplay '02)*, Nice, France, 2002 (unpublished), Vol. 2, p. 877.
- [8] P. Martinot-Lagarde, H. Dreyfus-Lambe, and I. Dozov, *Phys. Rev. E* **67**, 051710 (2003).
- [9] R. Barberi *et al.*, *Phys. Rev. Lett.* **93**, 137801 (2004).
- [10] L. Z. Ruan and J. R. Sambles, *Appl. Phys. Lett.* **86**, 052502 (2005).
- [11] P. D. Brimicombe and E. P. Raynes, *Appl. Phys. Lett.* **89**, 031121 (2006).
- [12] B. Yang, S. J. Elston, E. P. Raynes, and H. D. Shieh, *Appl. Phys. Lett.* **91**, 071119 (2007).
- [13] G. Lombardo *et al.*, *Phys. Rev. E* **77**, 020702(R) (2008).
- [14] P. G. de Gennes and J. Prost, *The Physics of Liquid Crystals* (Oxford University Press, Oxford, 1993).
- [15] C. H. Gooch and H. A. Tarry, *J. Phys. D* **8**, 1575 (1975).
- [16] A. V. Kachynski, A. N. Kuzmin, P. N. Prasad, and I. I. Smalyukh, *Appl. Phys. Lett.* **91**, 151905 (2007).
- [17] B. Chen and S. Lim, *Appl. Phys. Lett.* **94**, 171911 (2009).